

# Measurement of Ionization Produced by 254 eV<sub>nr</sub> Nuclear Recoils in Germanium

A.R.L. Kavner<sup>1,\*</sup> and I. Jovanovic<sup>1</sup>

<sup>1</sup>University of Michigan, Ann Arbor, MI, USA

(Dated: May 21, 2024)

The ionization or scintillation produced by low-energy nuclear recoils is the primary signature of dark matter. Despite the urgency of dark matter detection and the recent measurements of coherent elastic neutrino-nucleus scattering, detector response is still not well characterized across a variety of materials in the keV<sub>nr</sub> and sub-keV<sub>nr</sub> regime. We have re-performed a measurement of the ionization produced by monoenergetic 254 eV<sub>nr</sub> nuclear recoils in Ge with improved digital electronics and event tagging scheme. Our results indicate an ionization yield of  $66 \pm 5$  eV<sub>ee</sub> corresponding to a quenching factor of  $25 \pm 2$  %, greater than the 14 % predicted by Lindhard Model. This quenching enhancement would greatly improve the sensitivity of high-purity Ge detectors for both dark matter detection and measurement of neutrinos via coherent scattering.

## I. INTRODUCTION

### A. Dark Matter and Neutrino Detection with High Purity Germanium

Direct detection of dark matter is among the highest priorities in experimental cosmology and particle physics [1–3]. Measurement of dark matter requires detectors with sensitivity to low-energy nuclear recoils  $\lesssim 1$  keV<sub>nr</sub> as well as a good understanding of the quenching factor, defined as the fraction of nuclear recoil kinetic energy released as ionization and/or scintillation [4]. The necessity for accurate modeling of such nuclear recoils has increased with the recent direct detection of coherent elastic neutrino-nucleus scattering (CE $\nu$ NS) [5]. It has been shown that the choice of quenching factor model greatly affects the degree to which experimental data agrees with Standard Model predictions [5].

The application of high-purity germanium (HPGe) detectors for dark matter searches and other rare-event physics experiments has increased in popularity [6]. This trend is due in part to the commercial availability of multi-kilogram HPGe detectors with suitably low noise and low background [7–9]. Multiple collaborations have or plan to deploy HPGe detectors for experiments aimed at detecting dark matter or neutrinos via CE $\nu$ NS [7, 8, 10–17]. The CDEX collaboration is investigating the dark matter sensitivity of a 50 kg array of HPGe detectors [18]. Given these advancements, a dark matter search or CE $\nu$ NS experiment with 100 kg of detection material could be considered in the near future.

### B. Low-Energy Quenching Factor

A detailed understanding of detector response to low-energy nuclear recoils is a prerequisite for experiments aimed at measuring neutrinos via CE $\nu$ NS or discovering

dark matter and is quantified through the quenching factor [3, 4]. In crystals such as Ge, quenching can be modeled by the Lindhard model [19], but below  $\sim 10$  keV<sub>nr</sub>, a poor agreement is observed between experimental data and the Lindhard prediction in a variety of detector materials including Ge [4, 10, 20–32].

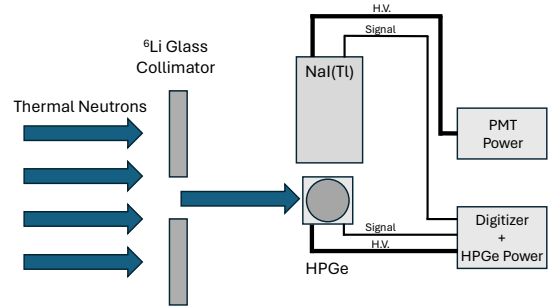


FIG. 1: Simplified diagram of the experimental setup. An HPGe detector was placed within the collimated neutron beamline, and a NaI(Tl) detector was placed on its side outside the neutron beam.

A recent multi-pronged study performed by the University of Chicago (UChicago) extensively studied the HPGe detector response to low-energy nuclear recoils and reported a significantly greater quenching factor than predicted by the Lindhard model in the sub-keV<sub>nr</sub> regime [19, 31]. Of particular interest is the measurement of the ionization produced by monoenergetic 254 eV<sub>nr</sub> <sup>73</sup>Ge nuclei. The UChicago study performed the same experiment as originally conducted by Jones and Kraner (Brookhaven) [23, 24] but reported a 44% greater ionization yield<sup>1</sup> [31].

To address this discrepancy, we have re-performed the measurement in the same setting as the UChicago study

<sup>1</sup> The value of 44 % is calculated using gamma-ray energy of 68.753 keV and values of 68.811 and 68.793 keV for the gamma-ray plus ionization produced by the nuclear recoil.

\* akavner@umich.edu

but with an improved experimental setup and procedure, utilizing multiple detectors, and modern digital electronics, and saving and analyzing raw detector waveforms. Our results corroborate the UChicago study [31], in disagreement with the earlier Brookhaven experiment [24].

### C. Level Structure of $^{73m}\text{Ge}$

In our experiment, 254 eV nuclear recoils are produced by the capture of thermal neutrons on  $^{72}\text{Ge}$  nuclei, comprising 27.4% of natural Ge, populating the 6785.2 keV excited state of  $^{73m}\text{Ge}$  [23, 24, 33]. The decay path of interest is depicted in Figure 2, where the majority of nuclear excitation is radiated via the emissions of 5852.2 keV or 5868.8 keV gamma rays that feed into the 915.2 keV or the 931.5 keV level, respectively. Only the 915.2 keV and 931.5 keV levels feed into the subsequent 68.75 keV state, which then decays to the ground state of  $^{73}\text{Ge}$  [23, 24, 33–35].

The de-excitation of  $^{73m}\text{Ge}$  results in nuclear recoils by conservation of momentum. Emission of the 5852.2 keV and 5868.8 keV gamma rays produces 253.5 eV<sub>nr</sub> and 252.1 eV<sub>nr</sub> nuclear recoil energies, respectively. The other gamma rays emitted contribute negligibly ( $\lesssim 1\%$ ) to the total nuclear recoil energy. A prior study [24] calculated the intensity-weighted average recoil energy of 254.1 eV<sub>nr</sub> with a spread of 1.5 eV<sub>nr</sub><sup>2</sup>. All gamma rays released in de-excitation of  $^{73m}\text{Ge}$ , except the lowest energy 68.75 keV gamma, have a high probability of escaping a small 2 cm<sup>3</sup> HPGe crystal<sup>3</sup> without interaction; their attenuation lengths in Ge are all longer than a centimeter. Attenuation lengths are calculated from the XCOM (NIST) database [36] and are listed in Table II.

Simulations in MCNPX [37] framework were used to model a uniform gamma-ray source emitted from a 1.6 cm (diameter)  $\times$  1.0 cm (height) cylindrical Ge crystal. The escape fraction, which we define as the fraction of gamma rays for a given emission line that does not interact with the crystal, either photoelectrically or by Compton scattering, is given in Table I. The combined probability that none of the gamma rays preceding the 68.75 keV level interact with the crystal is 30.35%, and the probability of a 68.75 keV gamma ray being photoelectrically absorbed within the crystal volume is 84.82%. The combined 68.75 keV gamma ray and nuclear recoil energy deposition is detected with an efficiency of 25.5%.

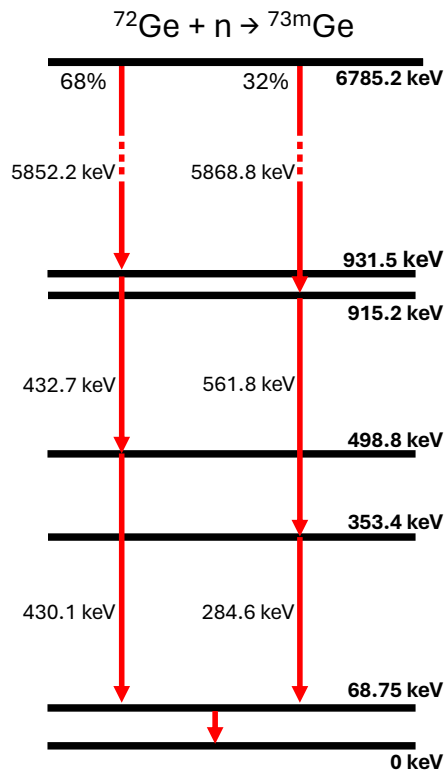


FIG. 2: De-excitation path of  $^{73m}\text{Ge}$  that feeds the 68.75 keV level. State energies are written on the right while gamma ray energies are written to the left of the red arrows designating the de-excitation path.

$E_\gamma$ [keV]	$E_{nr}$ [eV <sub>nr</sub> ]	Attenuation [mm]	Escape Fraction [%]
5868.8	253.5	60.4	91.3
5852.2	252.1	60.3	91.3
561.8	2.3	24.3	80.7
432.7	1.4	21.1	78.4
430.1	1.4	20.0	78.3
284.6	0.6	15.9	73.5
68.75	0.0	1.3	15.2

TABLE I: Emitted gamma rays from de-excitation of  $^{73m}\text{Ge}$  which decay to ground state via the 68.75 keV state. Attenuation lengths are calculated from the XCOM NIST database [36]. The escape fraction is defined as the fraction of gamma rays that do not interact with the crystal and is determined by Monte-Carlo simulation assuming a uniform source in a 2 cm<sup>3</sup> crystal used in the experiment.

### D. Prior Results

To the best of our knowledge, Refs. [24] and [31] are the only two prior measurements of combined energy deposition by the 68.75 keV gamma ray and the nuclear recoil. The ionization yield from 254.1 eV<sub>nr</sub> nuclear recoils can

<sup>2</sup> The calculation assumes rapid stopping of the  $^{73}\text{Ge}$  nucleus compared to the lifetimes of nuclear states.

<sup>3</sup> 1.6 cm diameter  $\times$  1 cm height is the crystal geometry of the Ortec GLP-16195/10P4 detector used in our experiment.

be calculated by subtracting the gamma-ray energy from the total measured energy. We adopt the gamma-ray energy of  $68.753 \pm 0.004$  keV, which is computed as an uncertainty-weighted arithmetic mean of prior measurements [23, 24, 31, 34, 38]

With this gamma-ray energy, the Brookhaven measurement yielded an electron equivalent nuclear recoil ionization energy of  $39$  eV<sub>ee</sub>, corresponding to a quenching factor of 15.5%. Subtracting the same gamma-ray energy from the UChicago result yields an ionization energy of  $58$  eV<sub>ee</sub>, corresponding to a quenching factor of 23%. The UChicago study adopts a gamma-ray energy of  $68.734$  keV which, when subtracted from their measured combined gamma and nuclear recoil energy deposition, yields a quenching factor of 30% [31]. The energy of gamma-ray significantly impacts the ionization yield, as demonstrated in Table II.

Regardless of the accepted value of the gamma ray, the UChicago result is significantly greater than the ionization predicted by Lindhard theory [19]. This discrepancy motivates additional study because such an enhanced quenching factor would significantly improve the sensitivity of HPGe detectors to low-energy recoils for dark matter and reactor CE $\nu$ NS detection.

Study	$\gamma$ + Recoil [keV]	$\gamma$ [keV]	Ionization [eV <sub>ee</sub> ]	Quenching [%]
Brookhaven	68.793	68.753	$39 \pm 5$	$15.4 \pm 2.1$
UChicago	68.811	68.734	$77 \pm 20$	$30.3 \pm 7.9$
Brookhaven	68.793	68.753	$39 \pm 5$	$15.5 \pm 2.1$
UChicago	68.811	68.753	$58 \pm 4$	$22.7 \pm 1.7$
Lindhard	-	-	36.2	14.3

TABLE II: Ionization yields and quenching factors are presented both as reported in [24, 31] and using a gamma ray energy of  $68.753$  keV. The Lindhard model prediction is based on a free parameter of  $\kappa = 0.157$  as theoretically predicted for Ge [19].

### E. Digital Electronics

The Brookhaven result is consistent with the predicted ionization yield from Lindhard model [19, 24] while the UChicago result is in tension [31]. To address the discrepancy, we repeated an experiment to measure the combined energy deposition by the  $68.75$  keV deexcitation gamma-ray and the nuclear recoil. Both prior experiments [24, 31] utilized traditional analog shaping amplifiers and multichannel analyzers, whereby only shaped pulse amplitude was recorded. In contrast, we measure time-coincident gamma-ray events in an HPGe and an external NaI(Tl) detector and save raw waveforms from both detectors. We measure the lifetime of the gamma cascade and perform a novel multi-shaping analysis from which we reject the hypothesis posed by UChicago group which states the difference between their results and the

Brookhaven result was caused by the difference in the time constants of their analog shaping amplifiers,  $8 \mu\text{s}$  and  $2 \mu\text{s}$  respectively, and the  $700$  ns lifetime of the  $68.75$  keV state [24, 31].

## II. EXPERIMENTAL METHODOLOGY

### A. Neutron Source

The experiment was deployed at the Ohio State University Nuclear Reactor Laboratory [39]. The reactor was operated at an estimated thermal neutron flux of  $1 - 2 \times 10^6$  cm<sup>-2</sup> s<sup>-1</sup> and was chosen for the high thermal purity of the neutron beam. The thermal neutron facility has been well characterized; only 3.76 neutrons in every 1000 delivered in the thermal beamline have energy above  $0.4$  eV [40]. Thermal neutron purity is critical as any momentum imparted by inelastic scattering will result in an erroneously high measurement of the quenching factor. The facility is the same one used in the UChicago study [31].

### B. Detectors and Data Acquisition

The experimental apparatus comprised two radiation detectors: the HPGe detector, which acted as the neutron beam target, and a large external scintillation detector to tag the emitted  $5.8$  MeV gamma ray. The HPGe detector was an Ortec GLP-16195/10P4 detector in PopTop configuration mounted on a multi-orientation portable cryostat [41, 42]. The HPGe crystal volume was  $2$  cm<sup>3</sup>, comparable in volume to the detector used in UChicago studies [31]. The outward-facing ion-implanted layer of the GLP detector is only  $0.3 \mu\text{m}$  thick and has negligible attenuation for externally incident X rays and gamma rays [31, 42, 43]. The GLP detector series is commonly used for measurement and spectroscopy of X rays and gamma rays with energies between  $1$  and  $200$  keV [43], an ideal match to the energy of interest in this experiment. The detector was placed in the reactor thermal neutron beamline as depicted in Figure 1. A <sup>6</sup>Li glass disc with a  $1$  inch diameter hole was used to collimate the beam and reduce activation backgrounds. A null measurement was performed by placing a different <sup>6</sup>Li disc with no hole, which completely blocked the beam port. A large  $3$  inch diameter,  $5$  inch long cylindrical NaI(Tl) scintillation detector was employed for coincident gamma tagging, also shown in Figure 1.

Both detector outputs were digitized at a rate of  $100$  MHz by a CAEN DT5780 module [44]. High-voltage bias and preamplifier power to the HPGe detector were provided by the same DT5780 unit. High voltage for the NaI(Tl) detector was provided by a separate CAEN DT5533E high-voltage module [45].

### C. Calibration

The energy scale was established using the 59.5409 keV gamma ray from  $^{241}\text{Am}$  and the  $\text{Pb } K\alpha_1$  and  $K\alpha_2$  X rays, 74.9694 keV and 72.8042 keV, respectively. A  $^{57}\text{Co}$  source and lead foil were used to produce X rays. The calibration sources were placed on top of a copper shim just above the beryllium window of the detector. The sources were present throughout the experiment to perform *in-situ* calibration and monitor for gain drift. No such drift was observed during the experimental runs, but the calibration changed by  $\sim 1\%$  from day to day as the detector was unbiased and re-biased over multiple days of measurements.

The relative timing between the HPGe and NaI(Tl) detectors was calibrated at the start, middle, and end of each day of the experiment. The energy scale in the NaI(Tl) detector was established with a  $^{60}\text{Co}$  gamma-ray source during the same periods. Continuous calibration was not performed with the NaI(Tl) detector as it would have caused an increased rate of spurious coincidences. Mid-day calibrations delineated the experiment into seven approximately equal-sized data sets. The runs were analyzed separately and the results averaged.

### D. Data Analysis

Raw preamplifier output waveforms were saved in 80  $\mu\text{s}$ -long traces. This allowed the same data to be processed and analyzed with multiple algorithms. Pulse amplitude was determined using three digital pulse shaping algorithms: the optimal filter [46–49], the trapezoidal filter, and a digitally synthesized CR-RC<sup>8</sup> Gaussian filter. The combined energy deposition by gamma ray and nuclear recoil was extracted from the optimally filtered data, while the other shaping filters facilitated quantification of the effect of analysis methodology on the result and comparison to prior studies.

Gaussian shaping filters are commonly implemented by analog shaping amplifiers [50, 51]. A Canberra (Mirion) 2022 NIM spectroscopy amplifier with a shaping time constant of 8  $\mu\text{s}$  was used in the UChicago experiment [31]. The amplifier used in the Brookhaven experiment [24] was not reported though the peaking time of 4  $\mu\text{s}$  was stated <sup>4</sup> [24]. As both prior studies utilized multichannel analyzers, the maximum of the Gaussian-shaped signal within the saved trace window is taken as the pulse energy <sup>5</sup> The waveforms were processed with multiple shaping time constants to test the hypothesis

that the choice of shaping time is the cause of the difference between the Chicago and Brookhaven results [24, 31].

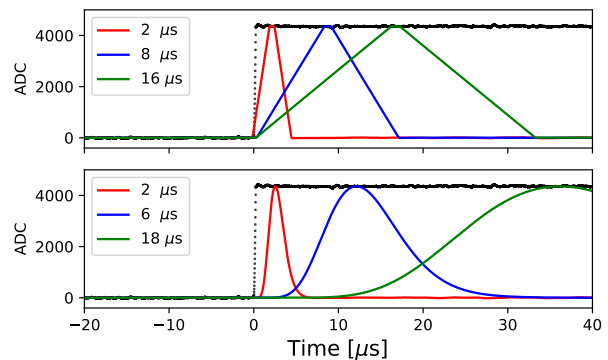


FIG. 3: Multiple shaping time trapezoidal and Gaussian (CR-RC<sup>8</sup>) filters applied to the same digitized waveform from the HPGe detector (black). For a given shaping time, the peaking time is longer for the Gaussian filter than for the trapezoidal filter. This is because, for the Gaussian filter, the shaping time corresponds to the RC and CR time constants while for the trapezoidal filter, it corresponds to a linear integrating window width.

The trapezoidal filter was also implemented as it is typically the filter of choice for HPGe signal analysis [50, 52, 53]. The filter is well characterized and has been digitally implemented since the mid-1990s [50, 52, 54, 55]. Three trapezoids with peaking times, of 2, 8, and 16  $\mu\text{s}$  were chosen to similarly test the effect of shaping time. An 800 ns flat-top time was chosen as it is sufficiently longer than the detector  $\sim 100$  ns (10–90%) rise time, such that ballistic deficit is minimized [50]. The amplitude of trapezoidally shaped signal was determined by sampling the middle of the flat top. The sample position was chosen by adding the associated peaking time and half the flat-top time to the pulse onset position. Sampling the flat-top is more robust to noise fluctuations than selecting the shaped signal maximum.

Minimal cuts were applied to the dataset in an attempt to not bias the result. Events were cut from the analysis based on saturation and pile-up. The effects of cuts within the energy range of interest are shown in Figure 4. The pile-up cut minimally affects the region around the 68.752 keV gamma ray. The region below 66 keV is significantly affected due to the 66.725 keV state, which decays by emission of 53.4 keV and 13.3 keV gamma rays, the latter having a half-life of 2.91  $\mu\text{s}$  [56–58].

## III. RESULTS

### A. Energy Spectrum

The best resolution was achieved with the optimally filtered data set. We use this dataset for primary analy-

<sup>4</sup> The peaking time of a Gaussian filter is typically 2–2.5 times longer than the shaping time constant [50, 51]

<sup>5</sup> The Brookhaven experiment does not explicitly report the use of a multichannel analyzer but it can be inferred as the x-axis units on their spectra are labeled in the units of channel number.

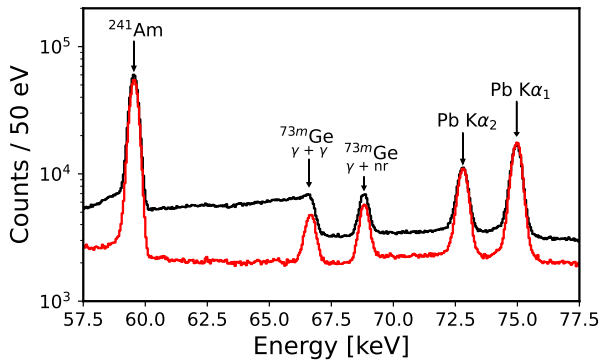


FIG. 4: Experimental energy spectrum in the energy range of interest with calibration and  $^{72}\text{Ge}$  ( $n,\gamma$ ) peaks labeled as acquired (black) and after pile-up cuts (red).

sis, while the trapezoidally filtered and Gaussian-shaped datasets were used for assessing the systematic contribution from the choice of pulse processing methodology.

In each of the data runs, the  $^{241}\text{Am}$  gamma peak and the  $\text{Pb } K\alpha_1$  and  $K\alpha_2$  X-ray peaks were fit with Gaussians modified by small correction functions based on [59]. The peak centroids were fit with a linear calibration function. These three peaks were chosen to provide the most accurate energy scale in the range of combined energy deposition by the 68.75 keV gamma ray and nuclear recoil and can be seen in Figure 4. The robustness of the energy scale was tested by performing an additional calibration using the 122 keV and 136 keV gamma-ray peaks. The change in scale was negligible compared to other uncertainties. The only feature strongly affected by the cuts is the aforementioned decay of the 66.7 keV state, which is not associated with the decay path of interest. The 66.7 keV peak was fit with an exponentially modified Gaussian functional form, the extracted energy from which was  $66.720 \pm 0.011$  keV, which agrees with the literature-reported value of  $66.725 \pm 0.009$  keV [34].

Thermal neutrons emitted from the beam port were verified to be the source of the signal. This was achieved by replacing the  $^6\text{Li}$  glass collimator with a solid  $^6\text{Li}$  glass disk for one three-hour data run. During this null measurement, the peak resulting from combined energy deposition of 68.75 keV gamma and nuclear recoil was not observed. Other peaks associated with neutron reactions on Ge observed during the data runs similarly were not seen or were seen at a significantly reduced rate during the null measurement.

## B. Energy Deposition

The peak attributed to the combined energy deposition of a 68.75 keV gamma ray and nuclear recoil is fit with

a Gaussian with a step to high energy:

$$f(x, \vec{\pi}) = \frac{A}{\sqrt{2\pi}\sigma} e^{-(x-\mu)^2/(2\sigma^2)} + \frac{B}{2} \cdot \text{erfc} \left[ \frac{\mu-x}{\sqrt{2}\sigma} \right]. \quad (1)$$

Parameters  $A$  and  $B$  are the area of the Gaussian and the amplitude of the step, respectively, while  $\mu$  and  $\sigma$  are the mean position and resolution. The step position and smearing of the rising edge are fixed to the same centroid and resolution as the peak as justified in [59, 60]. The fit to optimal filtered data spectrum peak with this functional form and the fit residual are shown in Figure 5.

We hypothesize the step structure to be formed when one of the gamma rays emitted prior to the 68.75 keV gamma ray and within the same gamma cascade Compton scatters within the crystal volume. In this scenario, energy deposited by the nuclear recoil, Compton electron, and the emitted and then photoelectrically absorbed 68.75 keV gamma ray is measured as a sum. This shifts the deposited energy higher and outside of the primary peak. To test this hypothesis, the Compton spectra from each of the preceding gamma rays in the energy region of 0–2 keV were simulated in the MCNP framework [37]. After accounting for the branching ratios and detection efficiency, the simulated ratio of the Compton spectrum amplitude to the combined gamma and nuclear recoil peak area was 0.125% whereas the ratio of best-fit  $A$  and  $B$  parameters yields  $0.16 \pm 0.01$  %. This functional form was found to fit the combined total data set well with a  $\chi^2/\text{ndf}$  value of 1.

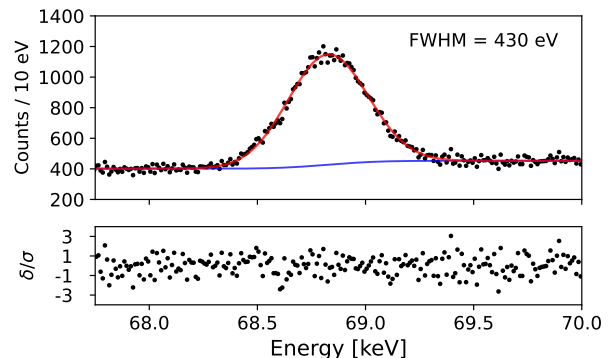


FIG. 5: Fit and residual to peak associated with the 68.75 keV gamma ray and nuclear recoil signal for all data sets. The red line shows the summed fit, Gaussian, baseline, and step while the blue trend is of the baseline and step components.

Each data set was fit with the functional form described in Eq. (1). The mean value, uncertainty of the mean, and calibration uncertainties are reported in Table III. The fit values were averaged using an inverse error-squared weighted arithmetic mean. The combined energy deposition by the gamma ray and the 254 eV<sub>nr</sub> nuclear recoil is  $68.816 \pm 0.002$  keV<sub>ee</sub>. Subtracting the gamma energy of 68.753 keV yields a nuclear recoil ion-

ization of  $62.7 \pm 4.7$  eV<sub>ee</sub>, corresponding to a quenching factor of  $24.6 \pm 1.8\%$ .

Run	$E_\gamma + E_{nr}$ [keV]	Fit [eV]	Slope [eV]	Intercept [eV]	Total [eV]
Run-1	68.8190	6.6	2.4	2.4	7.4
Run-2	68.8486	10.8	4.5	5.1	12.7
Run-3	68.8205	5.5	3.1	3.3	7.1
Run-4	68.8206	4.2	2.5	3.0	5.8
Run-5	68.8269	3.8	2.4	2.4	5.1
Run-6	68.7998	4.5	2.8	3.9	6.6
Run-7	68.8032	4.2	1.4	2.0	4.9
Combined	68.8159	1.8	0.9	1.1	2.4

TABLE III: Mean parameter of the Gaussian fit to the combined energy deposition from 68.75 keV gamma ray and nuclear recoil with associated uncertainties.

### C. Lifetime of Nuclear States

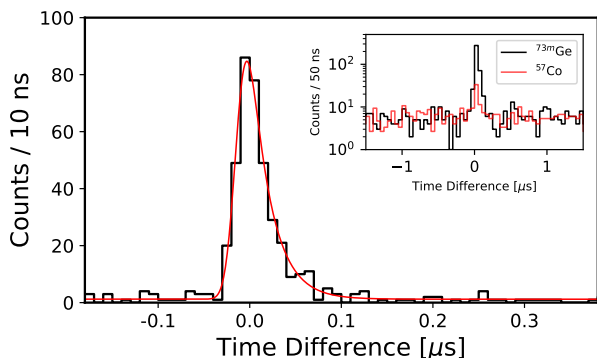


FIG. 6: Time difference distribution between HPGe and NaI(Tl) event after application of energy gating cuts to select events within the region of the combined energy deposition by 68.75 keV gamma and nuclear recoil in HPGe and greater than 4 MeV energy deposition in the NaI(Tl) detector. *Inset*: comparison with the 122 keV  $^{57}\text{Co}$  gamma peak to access the level of spurious and accidental coincidences.

The Brookhaven experiment reported the lifetime of the 68.75 keV state to be 700 ns, and the preceding states in the de-excitation cascade have sub-nanosecond lifetimes [24]. We define the *effective lifetime* of the 68.75 keV state as the sum of its lifetime and the lifetimes of the preceding 353 keV and 915 keV states (or 499 keV and 932 keV states, depending on the de-excitation path). This determines the delay between the nuclear recoil and the 68.753 keV gamma-ray signal within the HPGe detector. The UChicago study stipulates this 700 ns lifetime paired with the difference in time constants utilized in their shaping amplifiers to be

the root cause for the difference between their and the Brookhaven result [31].

The effective lifetime is measured by finding time-coincident pairs of events between the HPGe and NaI(Tl) detectors. Energy gating is enforced to accept only coincident events where between 68.4 keV and 69.3 keV was deposited in the HPGe detector and more than 4 MeV was deposited in the NaI(Tl) detector. A strong time-correlated signal is observed for the energy-gated events as shown in Figure 6; 373 coincident pairs were found between  $-100$  ns and  $200$  ns. We define two background populations – spurious and accidental coincident events. Spurious events are defined as randomly coincident events in HPGe and NaI(Tl) detectors originating from unrelated sources. This flat background is estimated to be 6 coincidence pairs per 100 ns. We define the accidental background as true coincident interactions between the two detectors, such as Compton scattering of external gamma rays that are not associated with the 68.75 keV emission from  $^{73}\text{Ge}$ . The accidental coincidence rate was estimated by applying a similar energy gate, 121.6 keV to 122.6 keV, around the 122 keV  $^{57}\text{Co}$  peak; 36 accidental coincident pairs were found after scaling for the peak area. Therefore, of the 373 time-tagged events, 319 originate from the  $^{72}\text{Ge}$  ( $n,\gamma$ ) reaction, resulting in a signal-to-background ratio of  $\sim 7:1$ .

A 100 MHz digitizer was selected for the experiment based on the expectation of a  $\sim 700$  ns state lifetime and was therefore sub-optimal for precisely measuring lifetimes shorter than several tens of ns. However, it can still be concluded that the lifetime is significantly shorter than 700 ns. The nuclear lifetime was evaluated by fitting the time difference distribution of coincident pairs to

$$f(x, \vec{\pi}) = \frac{A \cdot e^{-(x-\mu)/\tau}}{2} \cdot \text{erfc} \left[ \frac{\mu - x}{\sqrt{2}\sigma} \right]. \quad (2)$$

The nominal fit values found a FWHM of 24 ns with a tail time constant of 22 ns. After deconvolution of the inherent detector response, determined from the  $^{22}\text{Na}$  calibration data, the effective lifetime was found to be  $17.2 \pm 7.6$  ns. This effective lifetime is  $\sim 100$  times shorter than the shaping time constant utilized in the Brookhaven experiment and would have a negligible effect on their result. The shaping time argument is, therefore, insufficient to explain the difference between the UChicago and Brookhaven results.

### D. Energy of Time-Coincident Events

The combined energy deposition by the 68.75 keV gamma ray and nuclear recoil can be assessed directly from the saved time-tagged waveforms independent of the form of fit to the peak in a digitally shaped spectrum. The amplitude of time-coincident waveforms is averaged and found to be 68.814 keV with a standard mean error of 7 eV. The total uncertainty is obtained

by adding in quadrature the calibration slope and the intercept uncertainty of 0.9 eV and 1.1 eV, respectively. The combined uncertainties are shown in Table III. Additional uncertainty arises from 18 spurious coincident events, the contribution of which was estimated using a Monte Carlo simulation where the energy of 18 randomly selected waveforms was sampled from a flat energy distribution, and the mean was re-calculated. This was found to alter the average by 3 eV. A Gaussian distribution was also sampled but found to change the mean by less than 1 eV. The more conservative value of 3 eV was selected to represent this uncertainty. In contrast, the 36 accidental coincident events are not expected to alter the average of the waveform population. The requirement for a minimum of 4 MeV being deposited in the NaI(Tl) detector necessitates that any accidental coincident event originates from a high-energy gamma-ray interaction. The energy deposited within the narrow energy gate region, 68.4 keV to 69.3 keV, by comparatively high energy gamma rays can be approximated as a flat distribution. From this analysis, the energy of events known to be comprised of combined energy deposition by the 68.75 keV gamma ray and the 254 eV nuclear recoil are within the energy range of  $68.814 \pm 0.008$  keV<sub>ee</sub>. This value is in agreement with  $68.816 \pm 0.002$  keV<sub>ee</sub> found by spectral fitting and supports its adoption as our reported value.

### E. Multi-Shaping Analysis

To further study the hypothesis of the impact of shaping time on the reconstructed combined energy deposition by the 68.75 keV gamma ray and nuclear recoil, waveforms were shaped by trapezoidal and Gaussian filters with varying time constants. The data was analyzed with three trapezoidal shaping times, 2, 8, and 16  $\mu$ s, and four Gaussian shaping times, 2, 6, 12, and 18  $\mu$ s. For both the trapezoidal and Gaussian shaping filters and all time constants, the reconstructed combined energy deposition by the 68.75 keV gamma ray and nuclear recoil differed by less than 2 eV with one exception, the 12  $\mu$ s Gaussian filter, where the difference is still within  $2\sigma$  of the accepted value.

The results of the multi-shaping analysis are shown in Figure 7 with our accepted value from the optimal filter in black, trapezoidally filtered in blue, and Gaussian filtered in red. The results are compared against the Brookhaven [24] and UChicago [31] results. The multi-shaping analysis does not explicitly account for statistical nor other systematic effects, but it demonstrates that the investigated analysis methodology, shaping filters, and shaping time constants do not explain the difference between the more recent studies (this work and UChicago experiment [31]) and the earlier Brookhaven study [24]. This is further consistent with our measured lifetime of the relevant nuclear states, which decay on a time scale more  $\sim$ three orders of magnitude faster than the shap-

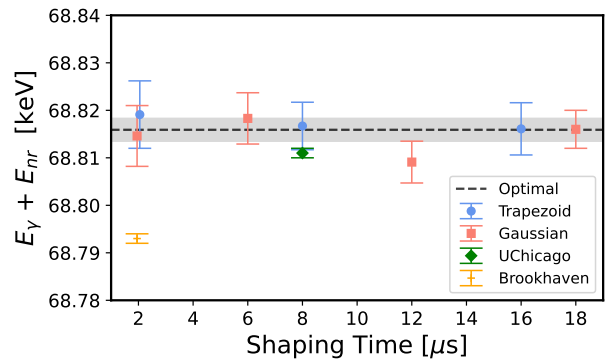


FIG. 7: Combined energy deposition by the gamma ray and nuclear recoil evaluated by optimal filter (black), trapezoidal filter (red), and Gaussian filter (blue) compared against the Brookhaven [24] and UChicago [31] results.

ing time constants utilized in this study as well as in Refs. [24, 31].

### F. Position Dependence

One potential systematic effect discussed in neither of the two previous studies is the possibility of a calibration offset caused by the difference in the average location of  $^{72}\text{Ge}(n,\gamma)$  events compared to the calibration sources. The combined 68.75 keV gamma and nuclear recoil signals are produced uniformly in the HPGe crystal whereas the  $^{241}\text{Am}$  gamma rays and Pb X rays predominantly interact near its top surface. We demonstrate no evidence for such position dependence through measurement of the decay of  $^{71}\text{Ge}$  produced in the crystal by neutron activation.

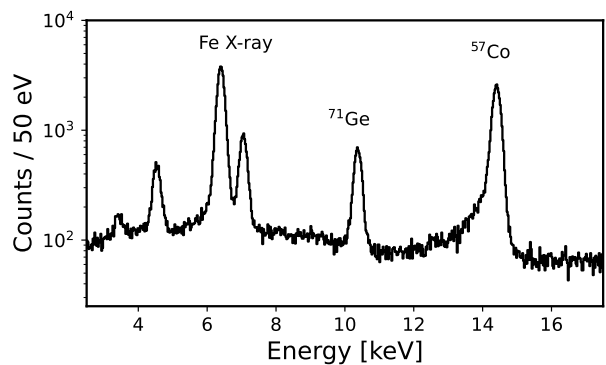


FIG. 8: Low-energy spectrum following neutron irradiation. The  $^{71}\text{Ge}$  10.37 keV peak is between the Fe X-ray peaks and the 14.4 keV gamma-ray peak, both from the  $^{57}\text{Co}$  calibration source.

Neutron irradiation resulted in HPGe detector activa-

tion by production of radioactive  $^{71}\text{Ge}$ , which decays via electron capture and emits 10.367 keV X rays corresponding to the K-edge of the daughter  $^{71}\text{Ga}$  [61–63]. Similarly to the combined energy deposition by the  $^{73m}\text{Ge}$  gamma ray and nuclear recoil, the  $^{71}\text{Ge}$  decays are uniformly distributed throughout the depth of the HPGe crystal. Following the neutron irradiation, we measured the 10.37 keV X rays, utilizing the 14.4 keV gamma ray, and 6.4 and 7.1 keV Fe X rays from  $^{57}\text{Co}$  for calibration. The  $^{71}\text{Ge}$  peak and calibration peaks analyzed with the same optimal filter analysis are shown in Figure 8. The  $^{71}\text{Ge}$  was fit with a Gaussian and a linear background term. The peak centroid was found to be 10.370 keV with a combined (fit and calibration) uncertainty of 4.4 eV. This value is within the uncertainty of both the accepted literature value of the  $^{71}\text{Ga}$  K-edge and the other measurements of  $^{71}\text{Ge}$  decay [61–65]. Were there a calibration offset between events near the surface and in the bulk of the crystal, the effect would be even more evident for the less penetrating 10.37 keV than for the 68.75 keV gamma rays. From this analysis, we conclude that no significant systematic offset exists due to the event position dependence.

## IV. DISCUSSION AND CONCLUSION

### A. Quenching Factor

The high level of agreement between our analysis methods shown in Figure 7 gives high confidence in the measured energy of the combined energy deposition by the 68.75 keV gamma ray and nuclear recoil of  $68.8159 \pm 0.0024$  keV. The appropriate gamma cascade is confirmed using an external tagging NaI(Tl) detector and the event time correlation. We further conclude the lifetime of the 68.75 keV state is significantly shorter than  $\sim 700$  ns suggested in [24]; this work finds the effective lifetime between nuclear recoil and gamma-ray signals of  $17.2 \pm 7.6$  ns.

As previously discussed, the ionization produced by the 254 eV<sub>nr</sub> nuclear recoil is calculated as the difference between the signal produced by combined energy deposition by the 68.75 eV gamma ray and nuclear recoil, and the energy of the nuclear level. The quenching factor is then calculated as the ratio of this difference and 254 eV. The accurate value for the energy of the gamma ray is therefore critical for determining the quenching factor, as summarized in Table II.

Given the various prior measurements summarized in Ref. [34, 35] we find it justifiable to accept an average gamma-ray value of  $68.7532 \pm 0.0040$  keV, from which we calculate quenching factor in Table IV<sup>6</sup>. We cannot rule

Study	$\gamma$ + Recoil [keV]	$\gamma$ [keV]	Ionization [eV <sub>ee</sub> ]	Quenching [%]
Brookhaven	68.793	68.753	$39 \pm 5$	$15.5 \pm 2.1$
UChicago	68.811	68.753	$58 \pm 4$	$22.7 \pm 1.7$
This Work	68.816	68.753	$63 \pm 4$	$24.7 \pm 1.8$

TABLE IV: Comparison of ionization yields and quenching factors calculated with the gamma-ray energy of 68.7532 keV.

out the possibility of some systematic offset that globally affected the measurements of the 68.75 keV nuclear level. However, this would not explain the disagreement between the Brookhaven study [24] and both this work and the UChicago study [31].

### B. Inter-Atomic Potential

The agreement between experimental data and the Lindhard model,  $\kappa = 0.157$ , observed above  $\sim 10$  keV<sub>nr</sub> but poor agreement observed near  $\sim 1$  keV<sub>nr</sub> [10, 20–32], suggest a significant modification in the quenching physics at the keV<sub>nr</sub> energy scale in Ge, which may be related to its material (crystalline) structure.

Both this work and the UChicago study [31] indicate a significant enhancement in the quenching factor in Ge above the Lindhard model. Ref. [31] postulates the Migdal effect as a potential explanation. However, more recent measurements find no Migdal nor Migdal-like signal in xenon [66]; as a result, any modification to Lindhard theory requires a material-dependent model. We hypothesize the inter-atomic potential plays a key role in the ionization produced by low-energy,  $\lesssim 1\text{--}2$  keV<sub>nr</sub> nuclear recoils. The stopping distance for a 254 eV<sub>nr</sub>  $^{73}\text{Ge}$  ion in Ge is of order 10 Å as discussed in Ref. [24]. This is the same length scale as the Ge lattice spacing, and hence the fundamental assumptions of Lindhard theory [19], notably that the ion travels through a homogeneous medium are not met. Furthermore, the vacancy site produced in the local lattice necessitates a change to the inter-atomic potential and band gap energy.

### C. Conclusion

This work reports a measured ionization yield of  $62.7 \pm 4.7$  eV<sub>ee</sub> from monoenergetic 254.1 eV<sub>nr</sub> Ge nuclear recoil. This corresponds to a quenching factor of  $24.7 \pm 1.8$  %, which confirms the 2021 UChicago study [31]. We have expanded upon it by tagging events known to be correlated with the emission of the 5.8 MeV gamma ray and hence must contain the signal from the 254 eV<sub>nr</sub> nuclear recoil. We have also shown the effective lifetime between the nuclear recoil and the decay of the 68.75 keV state to be shorter than  $\sim 700$  ns estimated in Ref. [24] and discussed in Ref. [31]. By saving raw pream-

<sup>6</sup> The UChicago ionization differs from their reported value that utilizes gamma-ray energy of 68.734 keV.



plier outputs, we demonstrated that shaping time and analysis methodology do not affect the result to the degree necessary to explain the discrepancy between the UChicago and Brookhaven studies. Lastly, by measuring the 10.37 keV signal from the decay of  $^{71}\text{Ge}$ , we have demonstrated no significant calibration offset originating from interaction position in the HPGe crystal. Accurate measurement of the energy of the 68.75 keV nuclear level of  $^{73}\text{Ge}$  is motivated as it impacts the quenching factor value and is also the leading source of uncertainty. However, broad systematic offsets would be required in the nuclear data [34, 35] to reconcile this work and the UChicago study with the Lindhard model.

## ACKNOWLEDGMENTS

This work was supported by the U.S. Department of Energy, Office of Nuclear Energy under DOE Idaho Op-

erations Office Contract DE-AC07-051D14517 as part of a Nuclear Science User Facilities experiment. This work was supported in part by the Department of Energy National Nuclear Security Administration, Consortium for Monitoring, Verification and Technology (DE-NE000863) and the Department of Energy National Nuclear Security Laboratory Research Graduate Fellowship. We thank the staff of the Ohio State University Nuclear Reactor Laboratory and William Heriot of the University of Michigan for their assistance in setting up and operating the experiment.

- 
- [1] R. Kolb, H. Weerts, N. Toro, R. V. de Water, R. Essig, D. McKinsey, K. Zurek, A. Chou, P. Graham, J. Estrada, J. Incandela, and T. Tait, Basic research needs for dark-matter small projects new initiatives: Report of the department of energy’s high energy physics workshop on dark matter 10.2172/1659757 (2018).
- [2] J. Feng, The WIMP paradigm: Theme and variations, *SciPost Phys. Lect. Notes*, 71 (2023).
- [3] R. Essig and et al., Snowmass2021 cosmic frontier: The landscape of low-threshold dark matter direct detection in the next decade.
- [4] J. Xu, P. Barbeau, and Z. Hong, Detection and calibration of low-energy nuclear recoils for dark matter and neutrino scattering experiments, *Annual Review of Nuclear and Particle Science* **73**, 95 (2023).
- [5] J. I. Collar, A. R. L. Kavner, and C. M. Lewis, Response of  $\text{cs}[na]$  to nuclear recoils: Impact on coherent elastic neutrino-nucleus scattering, *Phys. Rev. D* **100**, 033003 (2019).
- [6] N. Fourches, M. Zielińska, and G. Charles, High purity germanium: From gamma-ray detection to dark matter subterranean detectors, in *Use of Gamma Radiation Techniques in Peaceful Applications*, edited by B. A. Almayah (IntechOpen, Rijeka, 2019) Chap. 5.
- [7] J. Colaresi, J. I. Collar, T. W. Hossbach, A. R. L. Kavner, C. M. Lewis, A. E. Robinson, and K. M. Yocum, First results from a search for coherent elastic neutrino-nucleus scattering at a reactor site, *Phys. Rev. D* **104**, 072003 (2021).
- [8] H. Bonet and et al., Large-size sub-keV sensitive germanium detectors for the conus experiment, *The European Physical Journal C* **81**, The European Physical Journal C (2021).
- [9] P. Scovell, E. Meehan, S. Paling, M. Thiesse, X. Liu, C. Ghag, M. Ginsz, P. Quirin, and D. Ralet, Ultra-low background germanium assay at the Boulby underground laboratory, *Journal of Instrumentation* **19** (01), P01017.
- [10] P. Barbeau, J. Collar, and O. Tench, Large-mass ultralow noise germanium detectors: performance and applications in neutrino and astroparticle physics, *Journal of Cosmology and Astroparticle Physics* **2007** (09), 009.
- [11] C. E. Aalseth, P. S. Barbeau, J. Colaresi, J. I. Collar, J. Diaz Leon, J. E. Fast, N. E. Fields, T. W. Hossbach, A. Knecht, M. S. Kos, M. G. Marino, H. S. Miley, M. L. Miller, J. L. Orrell, and K. M. Yocum (CoGeNT Collaboration), Cogent: A search for low-mass dark matter using  $p$ -type point contact germanium detectors, *Phys. Rev. D* **88**, 012002 (2013).
- [12] R. Bonicalzi, J. Collar, J. Colaresi, J. Fast, N. Fields, E. Fuller, M. Hai, T. Hossbach, M. Kos, J. Orrell, C. Overman, D. Reid, B. VanDevender, C. Wiseman, and K. Yocum, The c-4 dark matter experiment, *Nuclear Instruments and Methods in Physics Research Section A: Accelerators, Spectrometers, Detectors and Associated Equipment* **712**, 27 (2013).
- [13] D. Akimov and et. al. **798**, 10.1088/1742-6596/798/1/012213 (2017).
- [14] K. Scholberg, Coherent elastic neutrino-nucleus scattering, *Journal of Physics: Conference Series* **1468**, 012126 (2020).
- [15] J. Colaresi, J. I. Collar, T. W. Hossbach, C. M. Lewis, and K. M. Yocum, Measurement of coherent elastic neutrino-nucleus scattering from reactor antineutrinos, *Phys. Rev. Lett.* **129**, 211802 (2022).
- [16] Z. Zhang and et. al. (CDEX Collaboration), Constraints on sub-gev dark matter–electron scattering from the cdex-10 experiment, *Phys. Rev. Lett.* **129**, 221301 (2022).
- [17] L. Singh, J. W. Chen, H. C. Chi, C.-P. Liu, M. K. Pandey, H. T. Wong, C. P. Wu, M. Agartioglu, M. Deniz, H. B. Li, S. T. Lin, V. Sharma, M. K. Singh, V. Singh, and Q. Yue (TEXONO Collaboration), Constraints on millicharged particles with low-threshold germanium detectors at kuo-sheng reactor neutrino laboratory, *Phys. Rev. D* **99**, 032009 (2019).
- [18] X. P. Geng and et. al., Projected sensitivity of the cdex-50 experiment (2023), arXiv:2309.01843 [hep-ex].
- [19] J. Lindhard, V. Nielsen, M. Scharff, and P. Thomsen, Integral equations governing radiation effects. (notes on

- atomic collisions, iii), Kgl. Danske Videnskab. Selskab. Mat. Fys. Medd. **33** (1963).
- [20] C. Chasman, K. Jones, and R. Ristinen, Measurement of the energy loss of germanium atoms to electrons in germanium at energies below 100 keV, Phys. Rev. Lett. **15**, 245 (1965).
- [21] C. Chasman, K. Jones, R. Ristinen, and J. Sample, Measurement of the energy loss of germanium atoms to electrons in germanium at energies below 100 keV. ii, Physical Review **154**, 239 – 244 (1967).
- [22] C. Chasman, K. Jones, H. Kraner, and W. Brandt, Band-gap effects in the stopping of  $ge^{72*}$  atoms in germanium, Phys. Rev. Lett. **21**, 1430 (1968).
- [23] K. W. Jones and H. W. Kraner, Stopping of 1- to 1.8-keV  $^{73}Ge$  atoms in germanium, Phys. Rev. C **4**, 125 (1971).
- [24] K. W. Jones and H. W. Kraner, Energy lost to ionization by 254-eV  $^{73}Ge$  atoms stopping in Ge, Phys. Rev. A **11**, 1347 (1975).
- [25] Y. Messous and et. al., Calibration of a Ge crystal with nuclear recoils for the development of a dark matter detector, Astroparticle Physics **3**, 361 (1995).
- [26] E. Simon and et. al., Sicane: a detector array for the measurement of nuclear recoil quenching factors using a monoenergetic neutron beam, Nuclear Instruments and Methods in Physics Research Section A: Accelerators, Spectrometers, Detectors and Associated Equipment **507**, 643 (2003).
- [27] A. Benoit and et. al. (EDELWEISS), Measurement of the response of heat-and-ionization germanium detectors to nuclear recoils, Nuclear Instruments and Methods in Physics Research Section A: Accelerators, Spectrometers, Detectors and Associated Equipment **577**, 558 (2007).
- [28] A. Ahmed and et. al. (CDMS Collaboration), Results from a low-energy analysis of the CDMS II germanium data, Phys. Rev. Lett. **106**, 131302 (2011).
- [29] A. Soma and et. al., Characterization and performance of germanium detectors with sub-keV sensitivities for neutrino and dark matter experiments, Nuclear Instruments and Methods in Physics Research Section A: Accelerators, Spectrometers, Detectors and Associated Equipment **836**, 67 (2016).
- [30] B. Scholz, A. Chavarria, J. Collar, P. Privitera, and A. Robinson, Measurement of the low-energy quenching factor in germanium using an  $^{88}Y/Be$  photoneutron source, Phys. Rev. D **94**, 122003 (2016).
- [31] J. Collar, A. Kavner, and C. Lewis, Germanium response to sub-keV nuclear recoils: A multipronged experimental characterization, Phys. Rev. D **103**, 122003 (2021).
- [32] A. Bonhomme, H. Bonet, C. Buck, J. Hakenmüller, G. Heusser, T. Hugle, M. Linder, W. Maneschg, R. Nolte, T. Rink, E. Pirovano, and H. Strecker, Direct measurement of the ionization quenching factor of nuclear recoils in germanium in the keV energy range, The European Physical Journal C **82**, 10.1140/epjc/s10052-022-10768-1 (2022).
- [33] M. A. Islam, T. J. Kennett, and W. V. Prestwich, Radiative strength functions of germanium from thermal neutron capture, Phys. Rev. C **43**, 1086 (1991).
- [34] B. Singh and J. Chen, Adopted levels, gammas for  $^{73}Ge$ , Nucl. Data Sheets **158** (2019), national Nuclear Data Center.
- [35] Iaea nuclear data services, <https://www-nds.iaea.org/relnsd/vcharthtml/VChartHTML.html>.
- [36] M. Berger, J. Hubbell, S. Seltzer, J. Chang, J. Coursey, R. Sukumar, D. Zucker, and K. Olsen, Xcom: Photon cross sections database, NIST Standard Reference Database 8 (XGAM).
- [37] L. Waters, G. McKinney, J. Durkee, M. Fensin, J. Hendricks, M. James, R. Johns, and D. Pelowitz, The mcnpX monte carlo radiation transport code, AIP Conference Proceedings **896**, 81 (2007).
- [38] G. Salzman, A. Goswami, and D. McDaniels, Coulomb excitation of  $^{73}Ge$  and quasiparticle-phonon coupling theories, Nuclear Physics A **192**, 312 (1972).
- [39] <https://reactor.osu.edu/>.
- [40] D. Turkoglu, J. Burke, R. Lewandowski, and L. Cao, Characterization of a new external neutron beam facility at the Ohio State University, Journal of Radioanalytical and Nuclear Chemistry **291**, 10.1007/s10967-011-1289-2 (2012).
- [41] <https://www.ortec-online.com/products/radiation-detectors/high-purity-germanium-hpge-radiation-detectors>.
- [42] <https://www.ortec-online.com/-/media/ametektortec/brochures/g/glp.pdf>.
- [43] F. Cannizzaro, G. Greco, M. Raneli, M. Spitale, and E. Tomarchio, A low-level spectrometer with a planar low-energy hpGe: shielding arrangement tests and system performance for 210pb determination in air filter samples, Applied Radiation and Isotopes **55**, 129 (2001).
- [44] (), <https://www.caen.it/products/dt5780>.
- [45] (), <https://www.caen.it/products/dt5533e>.
- [46] W. Press, S. Teukolsky, W. Vetterling, and B. Flannery, *Numerical Recipes in C*, 2nd ed. (Cambridge University Press, Cambridge, USA, 1992).
- [47] S. W. Smith, *The Scientist and Engineer's Guide to Digital Signal Processing* (California Technical Publishing, 1997).
- [48] Y. Yuryev, Y. Jang, S. Kim, K. Lee, M. Lee, S. Lee, W. Yoon, and Y. Kim, Nuclear Instruments and Methods **635**, 82 (2021), doi:10.1016/j.nima.2011.01.127.
- [49] G. S. F. C. A. S. Division, Xrs-2 pulse height analysis - details.
- [50] G. Knoll, *Radiation Detection and Measurement (4th ed.)* (John Wiley, Hoboken NJ, 2010).
- [51] Ortec, Introduction to amplifiers, <https://www.ortec-online.com/-/media/ametektortec/other/amplifier-introduction.pdf>.
- [52] IEEE standard test procedures for germanium gamma-ray detectors, IEEE Std 325-1996 10.1109/IEEESTD.1997.82400 (1997).
- [53] R. M. Keyser and T. R. Twomey, Optimization of pulse processing parameters for hpGe gamma-ray spectroscopy systems used in extreme count rate conditions and wide count rate ranges, Journal of Radioanalytical and Nuclear Chemistry **296**, 503 (2013).
- [54] V. T. Jordanov, G. F. Knoll, A. C. Huber, and J. A. Pantazis, Digital techniques for real-time pulse shaping in radiation measurements, Nuclear Instruments and Methods in Physics Research Section A: Accelerators, Spectrometers, Detectors and Associated Equipment **353**, 261 (1994).
- [55] V. T. Jordanov and G. F. Knoll, Digital synthesis of pulse shapes in real time for high resolution radiation spectroscopy, Nuclear Instruments and Methods in Physics Research Section A: Accelerators, Spectrometers, Detectors and Associated Equipment **345**, 337 (1994).

- [56] G. Czjzek, J. L. C. Ford, J. C. Love, F. E. Obenshain, and H. H. F. Wegener, Coulomb-recoil-implantation mössbauer experiments with  $^{73}\text{Ge}$ , *Phys. Rev.* **174**, 331 (1968).
- [57] L. Pfeiffer, R. S. Raghavan, C. P. Lichtenwalner, and A. G. Cullis, Mössbauer effect of the 13.3-keV transition in  $^{73}\text{Ge}$ , *Phys. Rev. B* **12**, 4793 (1975).
- [58] R. S. Raghavan and L. Pfeiffer, Observation of the high-resolution mössbauer resonance in  $^{73}\text{Ge}$ , *Phys. Rev. Lett.* **32**, 512 (1974).
- [59] L. Longoria, A. Naboulsi, P. Gray, and T. MacMahon, Analytical peak fitting for gamma-ray spectrum analysis with Ge detectors, *Nuclear Instruments and Methods in Physics Research Section A: Accelerators, Spectrometers, Detectors and Associated Equipment* **299**, 308 (1990).
- [60] G. W. Phillips and K. W. Marlow, Automatic analysis of gamma-ray spectra from germanium detectors, *Nuclear Instruments and Methods* **137**, 525 (1976).
- [61] A. Thompson and et. al., X-ray data booklet, <https://cxro.lbl.gov/x-ray-data-booklet>.
- [62] J. BEARDEN and A. BURR, Reevaluation of x-ray atomic energy levels, *Rev. Mod. Phys.* **39**, 125 (1967).
- [63] J. Fuggle and N. Martensson, Core-level binding energies in metals, *Journal of Electron Spectroscopy and Related Phenomena* **21**, 275 (1980).
- [64] C. Aalseth and et. al. (CoGeNT Collaboration), Results from a search for light-mass dark matter with a  $p$ -type point contact germanium detector, *Phys. Rev. Lett.* **106**, 10.1103/PhysRevLett.106.131301 (2011).
- [65] K. Ke-Jun and et. al., Cdex-1 1 kg point-contact germanium detector for low mass dark matter searches, *Chinese Physics C* **37**, 10.1088/1674-1137/37/12/126002 (2013).
- [66] J. Xu, D. Adams, B. Lenardo, T. Pershing, R. M. amd E. Bernard, J. Kingston, E. Mizrachi, J. Lin, R. Essig, V. Mozin, P. Kerr, A. Bernstein, and M. Tripathi, Search for the Migdal effect in liquid xenon with keV-level nuclear recoils 10.48550/arXiv.2307.12952 (2023).
- [67] S. Agostinelli and et. al., Geant4—a simulation toolkit, *Nuclear Instruments and Methods in Physics Research Section A: Accelerators, Spectrometers, Detectors and Associated Equipment* **506**, 250 (2003).
- [68] G. Škoro, I. Aničin, A. Kukoč, D. Krmpotić, P. Adžić, R. Vukanović, and M. Župančić, Environmental neutrons as seen by a germanium gamma-ray spectrometer, *Nuclear Instruments and Methods in Physics Research Section A: Accelerators, Spectrometers, Detectors and Associated Equipment* **316**, 333 (1992).
- [69] A. E. Chavarria, J. I. Collar, J. R. Peña, P. Privitera, A. E. Robinson, B. Scholz, C. Sengul, J. Zhou, J. Estrada, F. Izraelevitch, J. Tiffenberg, J. R. T. de Mello Neto, and D. Torres Machado, Measurement of the ionization produced by sub-keV silicon nuclear recoils in a CCD dark matter detector, *Phys. Rev. D* **94**, 082007 (2016).
- [70] F. Izraelevitch and et. al., *Journal of Instrumentation* **12** (06), P06014.
- [71] D. Z. Freedman, Coherent effects of a weak neutral current, *Phys. Rev. D* **9**, 1389 (1974).
- [72] M. Ibe, W. Nakano, Y. Shoji, and K. Suzuki, Migdal effect in dark matter direct detection experiments, *J. High Energy Phys.* **194**.
- [73] N. S. Bowden, Reactor monitoring and safeguards using antineutrino detectors, *Journal of Physics: Conference Series* **136**, 022008 (2008).
- [74] M. Andriamirado, A. B. Balantekin, and et. al. (PROSPECT Collaboration), Improved short-baseline neutrino oscillation search and energy spectrum measurement with the prospect experiment at hfr, *Phys. Rev. D* **103**, 032001 (2021).
- [75] L. Wen, J. Cao, and Y. Wang, Reactor neutrino experiments: Present and future, *Annual Review of Nuclear and Particle Science* **67**, 183 (2017).
- [76] D. Akimov and et. al., *Science* **357**, 1123 (2017).
- [77] A. Drukier and L. Stodolsky, Principles and applications of a neutral-current detector for neutrino physics and astronomy, *Phys. Rev. D* **30**, 2295 (1984).
- [78] L. Pfeiffer, Measurement of large  $e2$  dispersive interference in the high-resolution  $^{73}\text{Ge}$  mössbauer transition at natural linewidth, *Phys. Rev. Lett.* **38**, 862 (1977).
- [79] G. M. Temmer and N. P. Heydenburg, Coulomb excitation of medium-weight nuclei, *Phys. Rev.* **104**, 967 (1956).
- [80] R. E. Holland and F. J. Lynch, Lifetimes of excited states of nuclei with odd mass, *Phys. Rev.* **121**, 1464 (1961).
- [81] H. Ma, Y. Chen, Q. Yue, L. Wang, T. Xue, Z. Zeng, K. Kang, J. Cheng, Y. Li, J. Li, and Y. Li, Cdex dark matter experiment: Status and prospects, *Journal of Physics: Conference Series* **1342**, 012067 (2020).
- [82] D. Foreman-Mackey, D. W. Hogg, D. Lang, and J. Goodman, The mcmc hammer, *Publications of the Astronomical Society of the Pacific* **125**, 306–312 (2013).
- [83] J. Goodman and J. Weare, Ensemble samplers with affine invariance, *Communications in Applied Mathematics and Computational Science* **5**, 10.2140/camcos.2010.5.65 (2010).
- [84] <https://emcee.readthedocs.io/en/stable/>.
- [85] R. Weishaup and D. Rabenstein, *Zeitschrift für Physik A Hadrons and nuclei* **251**, 10.1007/BF01380454 (1972).
- [86] L. Baudis, J. Hellmig, H. Klapdor-Kleingrothaus, Y. .Rammachers, J. Hammer, and A. Mayer, High-purity germanium detector ionization pulse shapes of nuclear recoils, gamma-interactions and microphonism, *Nuclear Instruments and Methods in Physics Research Section A: Accelerators, Spectrometers, Detectors and Associated Equipment* **418**, 348 (1998).